International Journal of Astrobiology (2023), **22**:3 205–215
doi:10.1017/S1473550422000441

CrossMark
CAMBRIDGE UNIVERSITY PRESS

RESEARCH ARTICLE

Particle motion determines the types of bioaerosol particles in the stratosphere

Kenji Miki[1,2]

[1]Kyoto University Graduate School of Advanced Integrated Studies in Human Survivability, Nakaadachi-cho, Yoshida, Sakyo-ku, Kyoto 606-8306, Japan
[2]Keio University Faculty of Science and Technology, 3-14-1 Hiyoshi, Kohoku-ku, Yoohama-shi, Kanagawa 223-8522, Japan
Author for correspondence: Kenji Miki, E-mail: kmikikyoto@gmail.com

Received: 11 July 2022; **Revised:** 9 December 2022; **Accepted:** 12 December 2022; **First published online:** 09 January 2023

Key words: Bioaerosols, particles, simulated motion, stratosphere

Abstract
Bioaerosol particles in the stratosphere are topics of interest for aerobiological and astrobiological studies. Although various studies have succeeded in sampling bioaerosol particles in the stratosphere, limited research has been conducted to evaluate how and why these bioaerosol particles can lift up to as high as the stratospheric level. This study tested different driving forces acting on particles in the stratosphere in order to simulate the motion of particles with various bioaerosol characteristics. The findings show that small pollen-sized particles can scarcely levitate in the stratosphere, although spore-sized and dust particles attached to microorganisms such as bacteria or fungus might be able to do so.

Contents

Introduction

Bioaerosol particles in the stratosphere are of interest from aerobiological and astrobiological perspectives. Some previous studies have focused on bioaerosol particle sampling (Bryan *et al*., 2014, 2019) with the aim of developing sampling methods to determine the extent of biosphere sampling of bioaerosol particles in the stratosphere. Although bioaerosol particles have been found in the stratosphere, the mechanism by which these particles reach tens of thousands of meters above sea level is not fully understood. Previous studies reported the injection of tropospheric air to the stratosphere (Mote *et al*., 1996) or vertical diffusion of the air in the stratosphere (Mote *et al*., 1998). Some meteorological mechanisms, such as quasi-periodic oscillation or Brewer–Dobson circulation were reported to transport mass or momentum upwards in the stratosphere (Plumb, 2002; Butchart, 2014). However, these previous studies on troposphere–stratosphere transport focused on the transport of gas, which requires much less momentum compared with bioaerosol particles. Another study suggested that chemical aerosol particles are distributed in the lower stratosphere because of volcanic eruptions, biomass burning and dust. However, these particles only have the size of accumulation mode (0.1–1.0 μm) at altitudes as low as 12 km. These previous studies cannot fully explain how microorganisms as large as 10 μm, which are believed to be too large to reach the stratospheric level, were sampled in the stratosphere at an altitude of 41 km (Harris *et al*., 2002). Some previous studies concluded that it is highly possible that large microorganism particles in stratosphere originate from space (Wainwright *et al*., 2006; Alshammari *et al*., 2011).

In this study, we simulated vertical particle motion in the stratosphere using parameters that have been suggested to represent the main driving forces. The results revealed the physical characteristics of bioaerosol particles that could potentially stay within the stratospheric level, or be lifted up to the stratospheric level.

Materials and methods

Virtual particles with various physical characteristics of bioaerosol particles were simulated based on equation (19) of Miki (2020) with the addition of the vertical wind velocity, W, and the neglect of the gravitational effect of the sun. In the simulation, the motion of a particle was assumed to be governed by gravity, buoyancy, friction from the air and photophoretic force, which as discussed by Wainwright *et al*. (2006). The photophoretic force results from the temperature difference in the gas next to the particles that results from the difference in solar heating. For micron sized particles exposed to sunlight the photophoretic force can be 20% of the weight of the particle (e.g. Tehranian *et al*., 2001). The terminal velocity of a particle (V) is given by:

$$V = \frac{(\pi D_{ae}^3/6)(\rho_p - \rho_f)g - F_{\Delta\alpha} + F_{\Delta T}}{((C_D Re_p)/24)(3\pi\eta D_{ae})} - W, \tag{1}$$

where D_{ae} is the aerodynamic diameter of the particle; W is the vertical wind speed in the stratosphere; r is the radius of the particle; ρ_p is the density of the particle, assumed to be the same as water (1000 kg m^{-3}) based on the aerodynamic diameter; ρ_f is the density of air; $F_{\Delta\alpha}$ and $F_{\Delta T}$ are the photophoretic forces, which are driven by the difference in the thermal accommodation coefficient inside a particle and the thermal gradient of the particle, respectively; C_D is the drag coefficient; Re_p is the Reynolds number of the particle; and η is the viscosity of air.

The viscosity of air (η) was derived from the Sutherland's formula as:

$$\eta = \left(\frac{T}{T_0}\right)^{3/2} \times \frac{T_0 + 110.4}{T + 110.4} \times 1.7932 \times 10^{-5}, \tag{2}$$

where T_0 is the temperature at sea level and T is the temperature at each altitude, which was calculated as equation (3) using an approximate formula used in the US standard atmosphere (United States Committee on Extension to the Standard Atmosphere, 1976) as first introduced in Miki (2020).

$$T = 30.46 \times \sin\left(\frac{z - 34619.46}{28253.7}\pi\right) + 238.06. \tag{3}$$

Gryazin and Beresnev (2011) reported that in the stratosphere, vertical wind blows at a monthly average speed of approximately 5.0 mm s^{-1} in upward and downward directions and an annual average speed of approximately 1.0 mm s^{-1} in upward and downward directions. In this study, wind speeds were set as 5.0 mm s^{-1} (5.0×10^{-3} m s^{-1}) and 1.0 mm s^{-1} ($\pm 1.0 \times 10^{-3}$ m s^{-1}) in upward and downward directions, and 0 mm s^{-1} because the simulation duration significantly varied depending on the variable settings such as particle size or density.

Reynold's number (Re_p) was derived using the following equation:

$$Re_p = \frac{\rho_f (V + W) D_{ae}}{\eta}. \tag{4}$$

The density of air (ρ_f) varied depending on the altitude of the stratosphere, and for each altitude, ρ_f was calculated using equations (5) and (6):

$$\rho_f = \frac{M}{RT} P, \tag{5}$$

$$P(h) = P_0 \exp\left(-\frac{h}{H}\right), \tag{6}$$

where M is the molar mass of the air, R is the gas constant, P is the air pressure at each altitude and H is the scale height of the Earth's atmosphere (8432 m). The approximate formula for the drag coefficient (C_D) changed depending on the amplitude of the Reynold's number of the particle (Re_p) as shown in equations (7) and (8). These were first introduced by Oseen (1910).

When $Re_p < 1$:

$$C_D = \frac{24}{Re_p}, \tag{7}$$

and when $Re_p \geq 1$:

$$C_D = \frac{24}{Re_p}\left(1 + \frac{3}{16} Re_p\right). \tag{8}$$

The two types of photophoretic forces, $F_{\Delta T}$ and $F_{\Delta\alpha}$, were calculated using equations (9)–(14), which have been previously introduced (Rohatschek, 1996; Wurm and Krauss, 2008). It was assumed that $F_{\Delta T}$ works downwards and $F_{\Delta\alpha}$works upward (Keith, 2010).

$$F_{\Delta T} = F_* \frac{2}{(P/p_*) + (p_*/P)} \tag{9}$$

$$F_{\Delta\alpha} = \frac{1}{12 c_m} \frac{\Delta\alpha}{\alpha} \pi r^2 S \frac{1}{\left(1 + \frac{P}{p_*}\right)^2} \tag{10}$$

$$p_* = D\sqrt{\frac{2}{\alpha}\frac{3T}{\pi r}} \tag{11}$$

$$F_* = D\sqrt{\frac{\alpha}{2}}\frac{r^2 JS}{C_T} \tag{12}$$

$$D = \frac{\pi}{2}\sqrt{\frac{\pi}{3}\kappa\frac{c_m \eta}{T}} \tag{13}$$

$$c_m = \sqrt{\frac{8}{\pi}\frac{RT}{M}}, \tag{14}$$

where, F_* is the maximum force under pressure p_*, J is the asymmetric parameter, C_T is the thermal conductivity, κ is the thermal creep parameter, c_m is the average speed of the atmospheric molecule, α is the thermal accommodation coefficient and $\Delta\alpha$ is the difference in the thermal accommodation coefficient inside a particle.

https://doi.org/10.1017/S1473550422000441 Published online by Cambridge University Press

When S is the solar radiation intensity at each altitude,

$$S(L) = S_0(L)\exp\left(-\frac{kM}{R}P_0\int_z^{\infty}\frac{1}{T}\exp\left(-\frac{h}{H}\right)\mathrm{d}h\right), \tag{15}$$

where S_0 is the solar radiation at wavelength (L) and k is a coefficient.

From equation (15), the relationship between the solar radiation above the atmosphere and that on the Earth's surface is described as follows:

$$\frac{\Delta S}{S_0} = 1 - \exp\left(-35.74 \times \frac{kM}{R}P_0\right), \tag{16}$$

where ΔS is the difference between S_0 and the solar radiation above the atmosphere S_{earth}.

From equation (16), k is described as follows:

$$k(L) = \frac{R}{-35.74 \times MP_0}\ln\left(\frac{S_{\mathrm{earth}}}{S_0}\right). \tag{17}$$

When $E(h)$ is given as equation (18), the effective irradiance is derived as equation (19).

$$E(h) = P_0\int_z^{\infty}\frac{1}{T}\exp\left(-\frac{h}{H}\right)\mathrm{d}h \tag{18}$$

$$I_{\mathrm{E}} = \frac{1}{\pi}\int_0^{\infty} S_0(L)\exp\left(-\frac{kM}{R}E\right)\mathrm{d}L \tag{19}$$

Equation (19) can be approximated using the piecewise quadrature as equation (20)

$$I_{\mathrm{E}} = \frac{1}{\pi}\int_{L_i=0}^{\infty} S_0(L_i)\exp\left(-\frac{kM}{R}E\right)\Delta L \tag{20}$$

As the actual solar radiation data, ASTM G-173-03, the distributions of power obtained by the National Renewable Energy Laboratory (NREL) were used (https://www.nrel.gov/grid/solar-resource/spectra-am1.5.html 2022/10/27; Fig. 1a). As the radiation data are obtained discretely every 0.5 or 5.0 nm, the effective irradiance was approximately calculated using equation (21):

$$I_{\mathrm{E}} \approx \frac{\left(\sum_{L_i=L_1}^{L_2} S_0(L_i)\exp\left(-\frac{kM}{R}E\right)\Delta L_i + \sum_{L_i=L_1'}^{L_2'} S_0(L_i)\exp\left(-\frac{kM}{R}E\right)\Delta L_i\right)}{2\pi}, \tag{21}$$

where $L_1 = 280.0$, $L_2 = 3990.0$, $L_1' = 280.5$ and $L_2' = 3995.0$. The solar irradiance at each altitude was derived as Fig. 1(b).

The asymmetric parameter (J) and thermal creep parameter (κ) were set at the values $J = 0.5$ and $\kappa = 1.14$ under the assumption that particle surfaces perfectly absorb light, as described in a previous study (Wurm and Krauss, 2008). The thermal conductivity (C_{T}) and thermal accommodation (α and $\Delta\alpha$) depend on the characteristics of the particles and ambient air; these parameters of bioaerosol particles have not yet been studied. We assigned 0.3 and 0.9 values to α to account for low and high thermal accommodations, respectively, and 0 and 0.2 to $\Delta\alpha$. The values of thermal conductivity (C_{T}) were set as 0.1 and 10, respectively, to cover a broad range of high and low thermal conductivities. Lastly, in order to analyse bioaerosol particle motion in the stratosphere, the diameters of some

https://doi.org/10.1017/S1473550422000441 Published online by Cambridge University Press

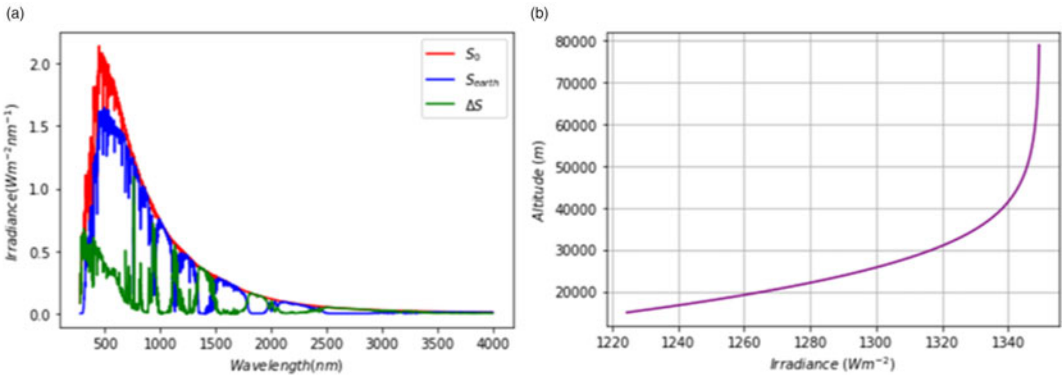

Fig. 1. *(a) Spectrum of solar irradiance at above the atmosphere (S_0), on the Earth's surface (S_{earth}), and the difference between S_0 and S_{earth} (ΔS). (b) Relationship between the altitude and the total irradiance.*

representative bioaerosol particles, such as pollen, spores and microorganisms, were selected as aerodynamic diameters in the simulation. For example, an aerodynamic diameter of 10 μm can be applied for small pollen grains because of various primary pollen taxa, such as small *Salix* pollen. Additionally, the maximum size of possible microorganism found in the stratosphere was found to be 10 μm (Harris *et al*., 2002; Wainwright *et al*., 2006), but was 2 μm in another study (Bryan *et al*., 2019). Spores were represented by a particle with an aerodynamic diameter of 1–3 μm based on a previous morphology study (Reponen *et al*., 2001). Thus, 1, 2, 5 and 10 μm were substituted as the representative aerodynamic diameters in this study.

In summary, every combination of the parameters given below were simulated.

$$W{:}[-5, -1, 0, 1, 5], D_{\mathrm{ae}}{:}[1, 2, 5, 10],$$
$$\alpha{:}[0.3, 0.9], \Delta\alpha{:}[0, 0.2], C_{\mathrm{T}}{:}[0.1, 10].$$

The initial altitude was set to 30 000 or 60 000 m, and the terminal velocity was adjusted every 3600 s based on the equations explained above at each altitude.

Results and discussion

The results of the particle vertical motion simulation calculated based on equation (1) showed that the relationship between $\Delta\alpha$ and solar radiation plays an important role in determining whether a particle in the stratosphere rises or falls when there is no vertical wind (e.g. Figs. 2–4(a) and (c)). When the particle diameter is 1 or 2 μm, the particle is uplifted and deposited when the wind blows upwards and downwards, respectively (Figs. 2 and 3). When the vertical wind speed is 0 mm s^{-1}, the particle is deposited when $\Delta\alpha$ is 0 though the particle is uplifted when $\Delta\alpha$ is 0.2, although if the particle is lifted or deposited is determined by the initial altitude only when the particle diameter is 2 μm, α is 0.9, $\Delta\alpha$ is 0.2 and C_{T} is 0.1 (Fig. 3(d)).

When the particle diameter is 5 μm, upward $F_{\Delta\alpha}$ is strong enough to carry the particle upwards regardless of a downward 1 mm s^{-1} wind (Fig. 4). In addition, the simulation results revealed that thermal conductivity influences particle motion when the particle size is 5 μm and when its magnitude was changed by two digits (Fig. 4(f)). Additionally, the body temperature of the particle, a variable of thermal accommodation and the colour of the particle seems to be largely influenced by the body temperature since the colour determines the solar radiation absorption rate of the particle.

The small pollen-sized particles (10 μm particles) struggled to levitate in the stratosphere unless the upward wind was strong enough and the ratio of the difference in the thermal accommodation

https://doi.org/10.1017/S1473550422000441 Published online by Cambridge University Press

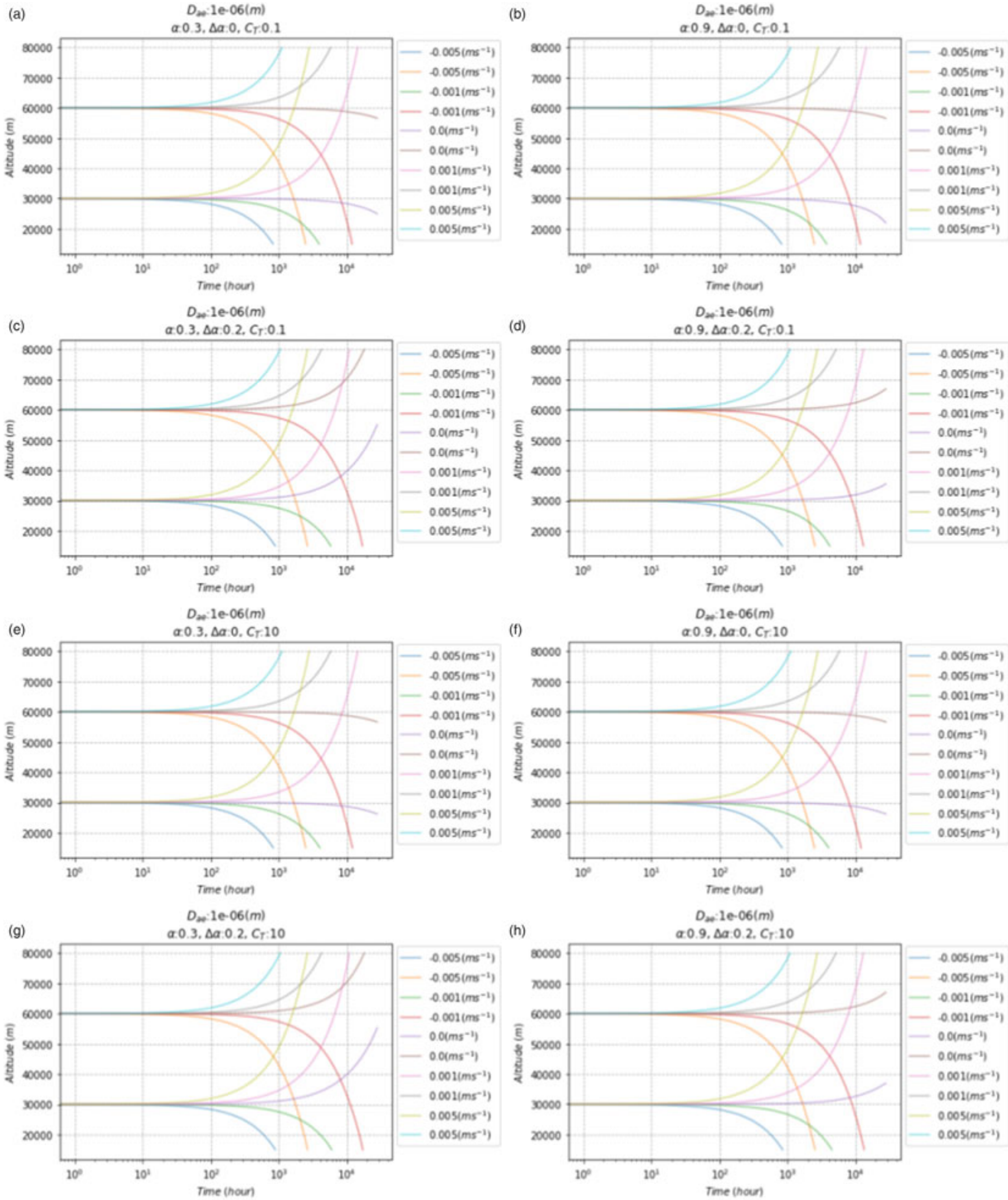

Fig. 2. *Simulation of bioaerosol particle motion in the stratosphere when the bioaerosol particle diameter is* 1×10^{-6} *m.*

coefficient inside a particle to the thermal coefficient of the particle itself was large (Fig. 5), although spore-sized particles always levitated when $\Delta\alpha$ was not zero. Thus, the results show that the 10 μm microorganisms found in a previous study could be from the Earth, assuming that the particle characteristics satisfy the conditions. Previous research has suggested that the morphology of a particle may influence the photophoretic force (Redding *et al.*, 2015). When the spore images available on the PAAA website (https://www.paaa.org/gallery/spores_eh/#) were analysed using ImageJ (Schneider *et al.*, 2012), the circularity of each spore (*Epicoocum*, *Curvularia* and *Spegazzinia*) was found to be:

https://doi.org/10.1017/S1473550422000441 Published online by Cambridge University Press

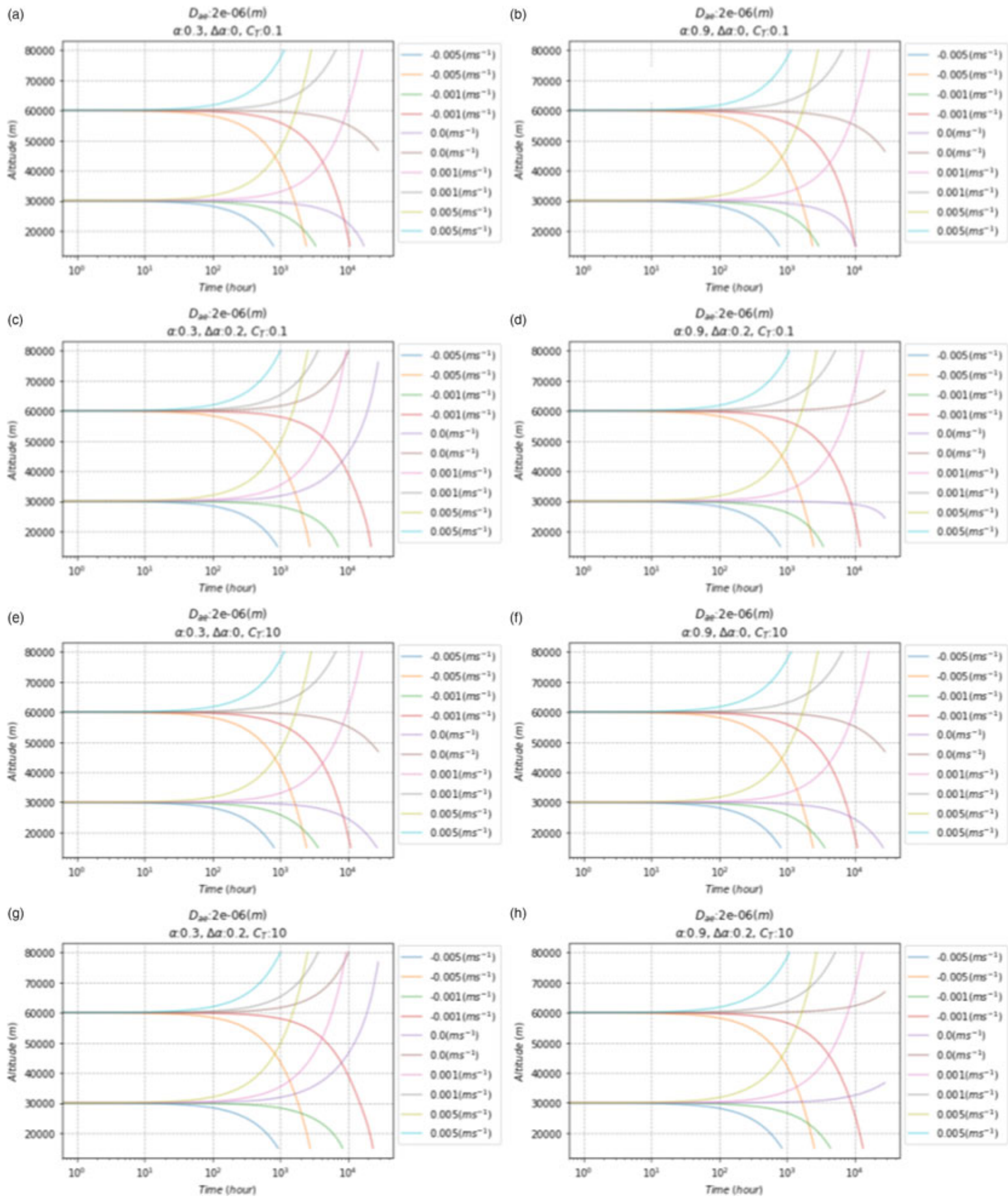

Fig. 3. *Simulation of bioaerosol particle motion in the stratosphere when the bioaerosol particle diameter is* 2×10^{-6} *m.*

Epicoocum: 0.843; *Curvularia*: 0.452; *Spegazzinia*: 0.669

Here, the circularity was derived using equation (22):

$$\text{circularity} = 4\pi\left(\frac{\text{Area}}{\text{Perimeter}^2}\right). \tag{22}$$

Thus, because some spores are not morphologically point-symmetric, the actual photophoretic force ($F_{\Delta\alpha}$) on them could be larger than that in the simulation. Although previous research indicated that a

https://doi.org/10.1017/S1473550422000441 Published online by Cambridge University Press

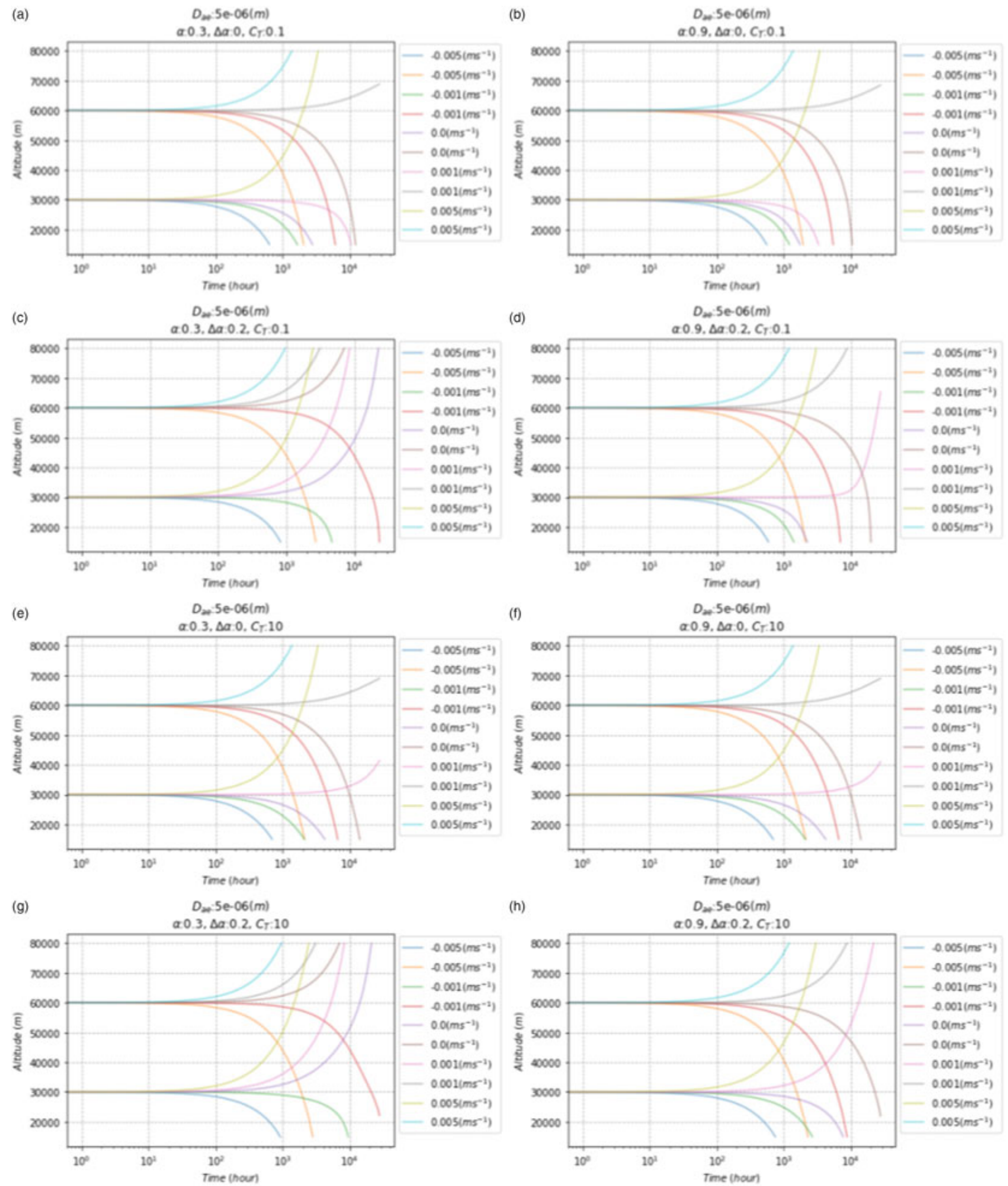

Fig. 4. *Simulation of bioaerosol particle motion in the stratosphere when the bioaerosol particle diameter is 5×10^{-6} m.*

particle with a diameter of 5 μm could possibly be uplifted into the stratosphere when only the uplifting wind is considered (Gryazin and Beresnev, 2011), the simulation in the present study, in which the photophoretic force was considered, showed that even a particle with a radius of 5 μm can be lifted when there is a difference in the accommodation coefficient of a particle or weak vertical uplift wind. This rise of a particle into the stratosphere appears to be identical to that of a microorganism attached to a dust particle (Barberán *et al.*, 2015; Hu *et al.*, 2020). This phenomenon has also been addressed in previous research (Wainwright *et al.*, 2006).

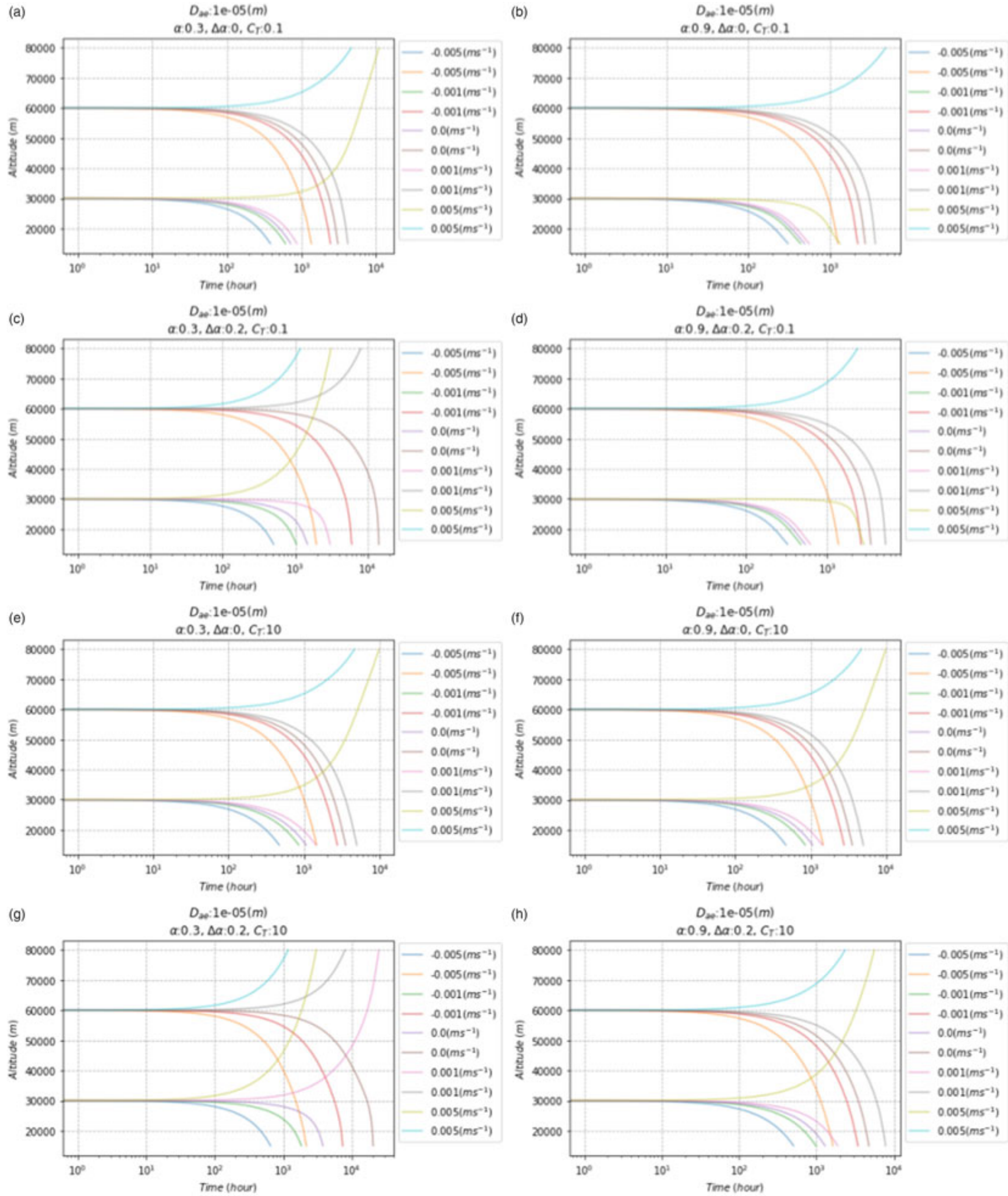

Fig. 5. *Simulation of bioaerosol particle motion in the stratosphere when the bioaerosol particle diameter is 1 × 10^{-5} m.*

In this study, bioaerosol particles were assumed to have a density of 1000 kg m^{-3} regardless of the particle type. However, Amaranthus pollen are reported to have a density of approximately 14 000 kg m^{-3} (Sosnoskie *et al*., 2009). Another previous study indicated that dry ragweed pollen has a density of 840 kg m^{-3}, but 1280 kg m^{-3} in 100% humidity environments (Harrington and Metzger, 1963). A previous study on spore particles assumed that a spore of *Gymnosporangium juniperi-virginianae* is 1200 kg m^{-3} (Fischer *et al*., 2010) while fungal spores of *Lycoperdon perlatum* have a density of 770 kg m^{-3} (Tesmer and Schnittler, 2007). Concerning dust particles, a dust particle in the Asian

https://doi.org/10.1017/S1473550422000441 Published online by Cambridge University Press

dust-storm theoretically has a density of 2600 kg m^{-3} (Iwasaki *et al*., 1983); however, because the chemical compounds vary significantly, the mass density will also vary significantly (Fergusson *et al*., 1986). Thus, understanding the motion of a specific type of particle in the stratosphere requires conversion of the geometric particle size to the aerodynamic particle size.

A previous study collected *Bacillus spp.* and *Penicillium* at an altitude of 20 km and found that cultured *Penicillium* had characteristic blue/green fruiting bodies with white mycelium (Smith *et al*., 2010). In order to understand the relationship between thermal accommodation and the uplifting force in the stratosphere, sampling the bioaerosol particles as they are and performing morphological analysis are important.

Although the results indicate that some types of bioaerosol particles can be lifted up to the high altitude (i.e. into the stratosphere), bioaerosol particles reported to be sampled in the stratosphere could have been contaminated. In addition, this study did not take into account global horizontal circulation of the stratospheric atmosphere and seasonal changes in the stratospheric environment. Previous research has suggested that the driving force by the electric field above thunderstorms can also be an uplifting force in the stratosphere (Dehel *et al*., 2008). Thus, performing more *in situ* bioaerosol sampling in the stratosphere and more multiple bioaerosol transportation simulations considering stratospheric phenomenon are required for a full understanding of stratospheric airborne ecology.

Conclusions

The simulation of various bioaerosol particles in the stratosphere showed the significance of a difference in thermal accommodation in determining particle motion changes for a diameter size of 5 μm. This shows that microorganisms such as fungus or bacteria attached to dust can possibly levitate in the stratosphere. In addition, 10 μm bioaerosol particles can be levitated when the morphological or physical characteristics are ideal. In contrast to Wainwright *et al*. (2006), these results suggest that 10 μm particles are not necessarily of extra-terrestrial origin and can be lifted from lower in the Earth' atmosphere.

Conflict of interest. None.

References

Alshammari F, Wainwright M, Alabri K and Alharbi SA (2011) Studies on ultrasmall bacteria in relation to the presence of bacteria in the stratosphere. *International Journal of Astrobiology* 10, 99–103. doi: 10.1017/S1473550410000364

Barberán A, Ladau J, Leff JW, Pollard KS, Menninger HL, Dunn RR and Fierer N (2015) Continental-scale distributions of dust-associated bacteria and fungi. *Proceedings of the National Academy of Sciences of the USA* 112, 5756–5761. doi: 10.1073/pnas.1420815112

Bryan NC, Stewart M, Granger D, Guzik TG and Christner BC (2014) A method for sampling microbial aerosols using high altitude balloons. *Journal of Microbiological Methods* **107**, 161–168.

Bryan NC, Christner BC, Guzik TG, Granger DJ and Stewart MF (2019) Abundance and survival of microbial aerosols in the troposphere and stratosphere. *The ISME Journal* **13**, 2789–2799.

Butchart N (2014) The Brewer-Dobson circulation. *Reviews of Geophysics* **52**, 157–184.

Dehel T, Lorge F and Dickinson M (2008) Uplift of microorganisms by electric fields above thunderstorms. *Journal of Electrostatics* **66**, 463–466.

Fergusson JE, Forbes EA and Schroeder RJ (1986) The elemental composition and sources of house dust and street dust. *Science of the Total Environment* **50**, 217–221.

Fischer MWF, Stolze-Rybczynski JL, Cui Y, Cui Y and Money NP (2010) How far and how fast can mushroom spores fly? Physical limits on ballistospore size and discharge in the Basidiomycota. *Fungal Biology* **114**, 669–675.

Gryazin VI and Beresnev SA (2011) Influence of vertical wind on stratospheric aerosol transport. *Meteorology and Atmospheric Physics* **110**, 15–162.

Harrington JB and Metzger K (1963) Ragweed pollen density. *American Journal of Botany* **50**, 532–539.

Harris MJ, Wickramasinghe NC, Lloyd D, Narlikar JV, Rajaratnam P, Turner MP, Al-Mufti S, Wallis MK, Ramadurai S and Hoyle F (2002) Detection of living cells in stratospheric samples. *Proceedings of SPIE* **4495**, 192–198.

Hu W, Murata K, Fan C, Fan C, Huang S, Matsusaki H, Fu P and Zhang D (2020) Abundance and viable of particle-attached and free-floating bacteria in dusty and nondusty air. *Biogeosciences (Online)* **17**, 4477–4487.

Iwasaki Y, Minoura H and Nagaya K (1983) The transport and special scale of Asian dust-storm clouds: a case study of the dust storm event of April 1979. *Tellus* **35B**, 189–196.

Keith DW (2010) Photophoretic levitation of engineered aerosols for geoengineering. *Proceedings of the National Academy of Sciences* **107**, 16428–16431.

Miki K (2020) Preliminary analysis of aerosol particle deposition in the middle atmosphere. *Earozoru Kenkyu* **35**, 273–278.

Mote PW, Rosenlof KH, McIntyre ME, Carr ES, Gille JC, Holton JR, Kinnersley JS, Pumphrey HC, Russell JM and Waters JW (1996) An atmospheric tape recorder: the imprint of tropical tropopause temperatures on stratospheric water vapor. *Journal of Geophysical Research. Atmospheres: JGR* **101**, 3989–4006.

Mote PW, Dunkerton TJ, McIntyre ME, Ray EA, Haynes PH and Russell JM (1998) Vertical velocity, vertical diffusion, and dilute by midlatitude air in the tropical lower stratosphere. *Journal of Geophysical Research. Atmospheres: JGR* **103**, 8651–8666.

Oseen CW (1910) Ober die Stokessche formel and uber die verwandte aufgabe in der hydrodynamik. *Arkiv for Mathematik, Astronomi och Fysik* **6**, 29.

Plumb RA (2002) Stratospheric transport. *Journal of the Meteorological Society of Japan* **80**, 793–809.

Redding B, Hill SC, Alexson D, Wang C and Pan YL (2015) Photophoretic trapping of airborne particles using ultraviolet illumination. *Optics Express* **23**, 3630–3639.

Reponen T, Grishpun SA, Conwell KL, Wiest J and Anderson M (2001) Aerodynamic versus physical size of spores: measurement and implication for respiratory deposition. *Grana* **40**, 119–125.

Rohatschek H (1996) Levitation of stratospheric and mesospheric aerosol by gravito-photophoresis. *Journal of Aerosol Science* **27**, 467–475.

Schneider CA, Rasband WS and Eliceiri KW (2012) NIH Image to ImageJ: 25 years of image analysis. *Nature Methods* **9**, 671–675.

Smith DJ, Griffin DW and Schuerger AC (2010) Stratospheric microbiology at 20 km over the Pacific Ocean. *Aerobiologia* **26**, 35–46.

Sosnoskie LM, Webster TM, Dales D, Rains GC, Grey TL and Culpepper AS (2009) Pollen grains size, density, and settling velocity for Palmer amaranth (*Amaranthu palmeri*). *Weed Science* **57**, 404–409.

Tehranian S, Giovane F, Blum J, Xu Y-L and Gustafson BÅS (2001) Photophoresis of micrometer-sized particles in the free-molecular regime. *International Journal of Heat and Mass Transfer* **44**, 1649–1657.

Tesmer J and Schnittler M (2007) Sedimentation velocity of myxomycete spores. *Mycological Progress* **6**, 229–234.

United States Committee on Extension to the Standard Atmosphere (1976) U.S. standard atmosphere, National Oceanic and atmospheric administration, Washington, p. 20.

Wainwright M, Alharbi S and Wickramasinghe NC (2006) How do microorganisms reach the stratosphere? *International Journal of Astrobiology* **5**, 13–15.

Wurm G and Krauss O (2008) Experiments on negative photophoresis and application to the atmosphere. *Atmospheric Environment* **42**, 2682–2690.